

# Diagnosing Human-object Interaction Detectors

Fangrui Zhu<sup>1</sup>, Yiming Xie<sup>1</sup>, Weidi Xie<sup>2</sup>, Huaizu Jiang<sup>1</sup>

<sup>1</sup>Northeastern University <sup>2</sup>Shanghai Jiao Tong University

{zhu.fang, xie.yim, h.jiang}@northeastern.edu, weidi@sjtu.edu.cn

## Abstract

Although we have witnessed significant progress in human-object interaction (HOI) detection with increasingly high *mAP* (mean Average Precision), a single *mAP* score is too concise to obtain an informative summary of a model’s performance and to understand why one approach is better than another. In this paper, we introduce a diagnosis toolbox for analyzing the error sources of the existing HOI detection models. We first conduct holistic investigations in the pipeline of HOI detection, consisting of human-object pair detection and then interaction classification. We define a set of errors and the oracles to fix each of them. By measuring the *mAP* improvement obtained from fixing an error using its oracle, we can have a detailed analysis of the significance of different errors. We then delve into the human-object detection and interaction classification, respectively, and check the model’s behavior. For the first detection task, we investigate both recall and precision, measuring the coverage of ground-truth human-object pairs as well as the noisiness level in the detections. For the second classification task, we compute *mAP* for interaction classification only, without considering the detection scores. We also measure the performance of the models in differentiating human-object pairs with and without actual interactions using the *AP* (Average Precision) score. Our toolbox is applicable for different methods across different datasets and available at <https://github.com/neu-vi/Diag-HOI>.

## 1. Introduction

Human-object interaction (HOI) detection aims to simultaneously detect the humans and objects, as well as understand their relationships from a static image. It provides structured interpretations of the semantics of visual scenes rather than just object recognition or detection. A successful HOI detection system is often an essential building block for many downstream applications, such as visual question answering [3, 1, 29, 24, 34, 24], image captioning [33, 2, 11, 18] and retrieval [8, 5, 26, 31, 27], etc.



Figure 1: **Illustration of the two sub-tasks in HOI detection.** (a) Detect all human and object boxes and identify human-object pairs that have interactions (person and snowboard). (b) Classify the interactions between them (hold, jump, ride, stand on, and wear).

In the recent literature, significant progress has been made on HOI detection [13, 7, 12, 32, 14, 43, 38, 39, 41, 20, 37, 36, 25, 19, 35, 42, 16, 23], as indicated by the rising *mAP* (mean Average Precision) scores on standard benchmarks. However, one critical issue is that such concise performance summaries are often not informative enough to understand the reason one approach outperforms another, or more importantly, how it could be improved. Generally speaking, the HOI detection consists of two sub-tasks: i) detecting pairs of interacting human and object (human-object pair detection) and ii) classification of their interactions<sup>1</sup>. These two tasks are not independent, but in a cascaded relationship, as shown in Fig. 1. The inaccurate detections will lead to inferior interaction classification, causing accumulated errors during the process.

In this paper, we introduce a diagnosis toolbox for detailed investigation of HOI detectors’ performance and provide quantitative break-down results of both the human-object pair detection and interaction classification tasks. We first perform a *holistic* analysis of the overall HOI detection accuracy. Inspired by the object detection diagnosis toolbox [4], we define a set of error types as well as oracles to fix them in the HOI detection pipeline across the human-object pair detection and interaction classification tasks. The *mAP* improvement, obtained by applying the oracle to each error, is used to measure the significance of

<sup>1</sup>We use ‘interaction’ and ‘action’ interchangeably.

different errors. The larger  $mAP$  improvement can be obtained for a particular type of error, the more it contributes to the failure of an HOI detector. We then delve into the human-object pair detection and interaction classification tasks, respectively, and conduct detailed studies. For the detection task, we mainly investigate the recall to see if it can detect all the ground-truth human-object pairs for the later stage of interaction classification. We also check the precision to check the noisiness level of the detections. For the interaction classification task, which is a multi-label classification problem, we compute the  $mAP$  for different interaction categories without considering the detection scores. Moreover, an HOI model also needs to differentiate negative detections, where the detected human-object pairs have no actual interactions, from positive ones (*i.e.*, with actual interactions). To diagnose such a binary classification problem, we report the  $AP$  (Average Precision) score.

With both such holistic and detailed investigations of the human-object pair detection and interaction classification, our toolbox provides a comprehensive diagnosis report for HOI detection models. To our best knowledge, this is the first toolbox dedicated for diagnosing errors for HOI detection in static images.

**Diagnosis findings.** Here, we highlight a few significant findings using our diagnosis toolbox.

- For both one-stage and two-stage approaches, most of the errors are from two sources: incorrect localization of the object in a human-object pair and incorrect interaction classification even if the localization is correct.
- Generally, two-stage approaches tend to have higher precision for the human-object pair detection task, meaning less noise in the detection. The recall is roughly the same as one-stage detector.
- However, none of the two-stage nor one-stage approaches' recall value is high enough ( $<84\%$ ) on the challenging HICO-DET benchmark. It shows that the human-object pair detection is a bottleneck.
- The  $mAP$  scores of the interaction classification for correctly localized human-object pairs show that one-stage approaches tend to perform better.
- However, for the binary classification task of differentiating the negative and positive human-object pairs (*i.e.*, with and without actual interactions), two-stage models tend to perform better.
- Both HICO-DET and V-COCO share similar error sources, *e.g.*, false positives are more prominent than false negatives. But the human-object pair recall on V-COCO is significantly higher meaning more ground-truths can be detected and the interaction classification is also easier on V-COCO, partly due to the smaller set of interaction categories.

Our diagnosis toolbox is applicable to different methods across different datasets. We hope our work can foster the

future development of HOI detection models.

## 1.1. Related Work

There are several analysis tools for object detection [21, 15, 4]. The seminal work [15] shows how to analyze the influences of object characteristics on detection performance and the impact of different types of false positives. But it requires extra annotations to help analyze the impacts of object characteristics, which is unlikely to be scalable in large-scale benchmark datasets. TIDE [4] improves the default evaluation tool provided by the COCO dataset [21]. It provides a more general framework for quantifying the performance improvement for different false positive and false negative errors in object detection and instance segmentation algorithms. Our quantitative analysis of different errors and different tasks in HOI detection is motivated by TIDE [4]. But unlike object detection, the coupled nature of human-object pair detection and interaction classification makes the analysis not trivial.

A similar error diagnosis work [10] is proposed for the video relation detection task, which adopts a similar holistic approach inspired by TIDE [4]. In our diagnosis toolbox, we go beyond the holistic error analysis and also conduct detailed investigations in two different sub-tasks of HOI detection, considering the cascade nature of the HOI detection pipeline. In [13], the authors also define several error types of false positives. However, the definition is specifically tailored for the annotation format of the V-COCO dataset, which is not applicable to others. In contrast, our analysis is applicable to different benchmark datasets. In [17], the authors analyze a specific issue of HOI detection, the long-tail problem of HOI categories and points out limiting factors. [22] proposes a new metric to advance HOI generalization, preventing the model from learning spurious object-verb correlations. Both [17] and [22] are complementary to our diagnosis tool and analysis results.

## 2. Preliminaries

### 2.1. Definition of HOI Detection

Given an input image  $I$ , the output of an HOI detector is a set of triplets  $\mathcal{S} = \{(b_i^h, b_i^o, a_i)\}_{i=1}^K$ , where  $b_i^h$ ,  $b_i^o$ , and  $a_i$  denote the  $i$ -th human bounding box, object bounding box, and their interaction class, respectively. Both  $b_i^h$  and  $b_i^o$  contain the coordinates of the bounding boxes as well as the category labels associated with them.  $K$  is the number of triplets. In essence, the HOI detection problem consists of two sub-tasks, as shown in Fig. 1. Firstly, it is required to correctly localize every human-object pair in interaction. Unlike the regular object detection problem, the localization task here is to associate a pair of human and object boxes. We then need to recognize their interaction labels. Note that, there may be multiple interactions associated with the

same human-object pair, making it a multi-label classification problem. For instance, the action of a person and a frisbee can be both `catch` and `hold`.

## 2.2. Computing $mAP$

For an output triplet  $(b_i^h, b_i^o, a_i)$  from a model, it is compared with all the ground-truth annotations, and considered to be a true positive (TP) of a HOI class if *all* the following conditions are satisfied:

- The category labels of the human and object bounding boxes are both correct.
- The intersection-over-union (IoU) w.r.t. the ground-truth annotations of the human  $\text{IoU}^h$  and object  $\text{IoU}^o$  both exceed 0.5, *i.e.*,  $\min(\text{IoU}^h, \text{IoU}^o) > 0.5$ .
- The predicted interaction label  $a_i$  is correct.

If *any* of them is not satisfied, it is considered as a false positive (FP). If multiple HOI predictions are matched to the same ground-truth human-object pair, the one with the highest confidence score, which is defined as the product of confidence scores of  $b_i^h$ ,  $b_i^o$ , and  $a_i$ , is chosen to be a TP while all others are considered as FPs.

All predicted triplets are collected from all the images in a benchmark for each HOI category. The detected triplets are sorted by descending the confidence scores. For each HOI category, given a threshold of the triplet confidence  $\tau_t$ , the cumulative precision and recall are defined as

$$P = \frac{N_{TP}}{N_{TP} + N_{FP}}, \quad R = \frac{N_{TP}}{N_{GT}}, \quad (1)$$

for those triplets whose confidence scores are greater than  $\tau_t$ .  $P$  denotes the precision and  $R$  is the recall.  $N_{TP}$ ,  $N_{FP}$ , and  $N_{GT}$  are the number of TPs, FPs, and ground-truth triplets in a particular HOI category. By varying the confidence threshold  $\tau_t$ ,  $P$  is interpolated such that it decreases monotonically, and  $AP$  (Average Precision) is computed as the integral under the precision-recall curve. Finally,  $mAP$  is defined as the average  $AP$  over all HOI categories.

## 2.3. Two-stage vs. One-stage HOI Detectors

Existing HOI detectors can be roughly grouped into two categories: two-stage and one-stage, as illustrated in Fig. 2. Two-stage HOI detectors first detect individual object instances, yielding a set of human and object bounding boxes, whose confidence scores must be greater than a *fixed* threshold  $\tau_d$ . Every single pair of human and object bounding boxes will then be *exhaustively* paired for action classification in the second stage, where the feature representations for the classification are from the object detector. Depending on the choice of the object detector, NMS (non-maximum suppression) may be adopted to remove duplicate object detections so there are no more duplicates in the human-object pairs and the final triplet outputs.

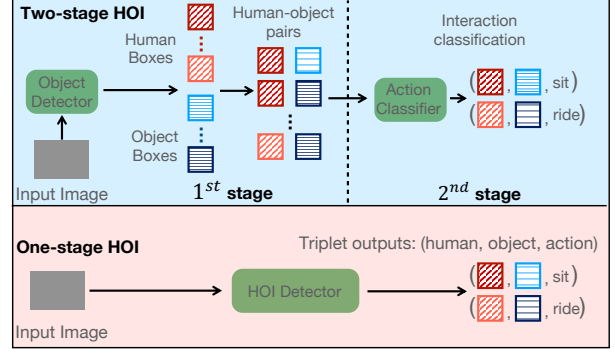


Figure 2: **Illustration of two- and one-stage HOI detectors.** The two-stage HOI detectors separate human-object pair detection and interaction classification, while one-stage ones model them as a triplet and directly output pairs with their interactions.

As for one-stage methods, the human-object pair detection (localization) and action classification are performed together without clear separation, where the feature representations are shared for both tasks. A one-stage detector directly localizes the human-object pairs that may have interactions and classifies the actions between humans and objects. NMS is usually adopted to remove duplicates in the final output of detected triplets.

Both two paradigms are being actively investigated. One-stage detectors usually run faster than their two-stage counterparts since skip the individual object detection and couple the human-object pair detection and action classification together to train a model. But in terms of accuracy ( $mAP$ ), there is no clear advantage for one over the other.

## 2.4. Benchmark Datasets

HICO-DET [7] and V-COCO [13] are two widely used benchmark datasets, both of which share the same 80 object categories as in the COCO dataset [21]. HICO-DET has 117 action classes, leading to 600 HOI categories (some combinations of objects and actions are not feasible). In V-COCO, there are 26 interaction classes. For each interaction, objects are annotated in three different roles: the agent, the instrument, or the object. The task is to detect the agent (human) and the objects in various roles for the interaction (*e.g.*, `<person cut_instrument knife>`, `<person read_object book>`).

## 2.5. On the `no_interaction` Class in HICO-DET

HICO-DET [7] is an extension of the HICO dataset [8] that focuses on image-level HOI classification only. In the HICO dataset, the `no_interaction` label is used to indicate that *none* of the human-object pairs within the image have interactions. Each of the 80 object categories is asso-

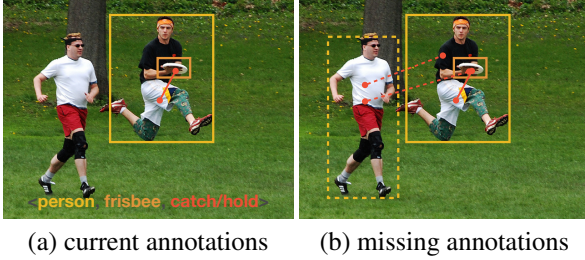


Figure 3: **An example of the missing annotations of the no\_interaction HOI class.** On the right, we show missing no\_interaction labels and missing bounding box using dashed lines and bounding boxes, respectively.

ciated with a no\_interaction action label, resulting in a total of 80 no\_interaction HOI classes.

HICO-DET inherits the 80 no\_interaction HOI classes in the detection setting, which consists of both localization and classification. However, it results in inconsistencies between the ground-truth annotations and the evaluation protocol w.r.t. the localization sub-task. To compute the  $mAP$  for the no\_interaction classes, all human-object pairs that have no interactions must be exhaustively annotated. Fig. 3 shows an example of the annotations for the no\_interaction HOI classes (including both missing bounding boxes and action labels). As a result, even if a model correctly outputs the no\_interaction labels, they will be considered as false positives and the  $mAP$  gets penalized. Note this is not an issue for the HOI classification in HICO [8] as no localization is needed.

How can we solve this issue? Obviously, exhaustively annotating all the missing no\_interaction human-object pairs is not feasible nor scalable. In fact, the no\_interaction HOI category is not needed. If there are no annotations stating that two objects have any *actual* interactions (e.g., catch or ride), it means they have no interactions as what the current annotations indicate in Fig. 3. This setting is adopted in the V-COCO [13] benchmark. Therefore, in our diagnosis, we remove all 80 no\_interaction HOI classes and only consider the remaining 520 ones in the HICO-DET benchmark [7].

### 3. Our Diagnosis Toolbox

#### 3.1. Error Analysis via $mAP$ Improvement

A useful way of diagnosing a method is to investigate the error patterns in its output. As we can see in Section 2.2, an HOI model can make errors in many places (e.g., human-object pair localization, action classification), leading to more FPs and fewer TPs (and thus lower  $mAP$ ). Inspired by the diagnosis method of object detection [4], we first define a set of error types of HOI detection, including both the

false positives and false negatives, as shown in Fig. 4. We then quantify the importance of each error by checking how much  $mAP$  improvement could be obtained if such an error could be perfectly solved.

**Human-object Pair Detection Errors.** We define the following set of error types at the level of the human-object pair.

- **Human box error:** The detected object bounding box is correct, but the human bounding box is incorrect (either incorrect localization where  $IoU^h < 0.5$ , or incorrect classification of the human label, or both).
- **Object box error.** The detected human bounding box is correct but the object bounding box is incorrect (either incorrect localization where  $IoU^o < 0.5$ , or incorrect classification of the object label, or both).
- **Both boxes error:** Neither the detected human nor object bounding box is correct.
- **Association error:** Both the human and object bounding boxes are correct, but they have no actual interaction.

**Action Classification Errors.** For the action classification, a human-object pair that has interaction has been correctly localized. The action classification errors are defined as follows.

- **Duplicate error:** The output action label is correct, but there is another detected triplet with a higher confidence score that has already matched to the ground truth.
- **Action error:** The output action is different from the ground-truth label.

**Missed GT Error.** A ground truth triplet is missing in the output and also not covered by any of the above errors. Such triplets will be considered as missed GT.

**Other Error Types.** We further make a clear split between false positive and false negative. The error types mentioned above account for all errors in the model, however, they do not provide a clear distinction between false positives and false negatives (pair detection and action classification errors can all capture false negatives). In situations where a clear differentiation is necessary, we introduce two distinct types of errors – false positive and false negative.

Among all such errors, one may wonder which one is more critical toward improving the  $mAP$  of HOI detection. To this end, we compute the improvement of  $mAP$  by fixing each error type with an oracle as follows.

$$\Delta mAP_o = mAP_o - mAP, \quad (2)$$

where  $mAP_o$  denotes the  $mAP$  score after applying the oracle  $o$  to fix an error type. The larger the  $\Delta mAP_o$  we can see for an error, the more important it is. Due to the space limit, we provide details about the oracles for fixing different errors in the supplementary material.

By examining the  $mAP$  improvement over different error types, we can better understand how false positives and false negatives affect the final  $mAP$  in a holistic manner.



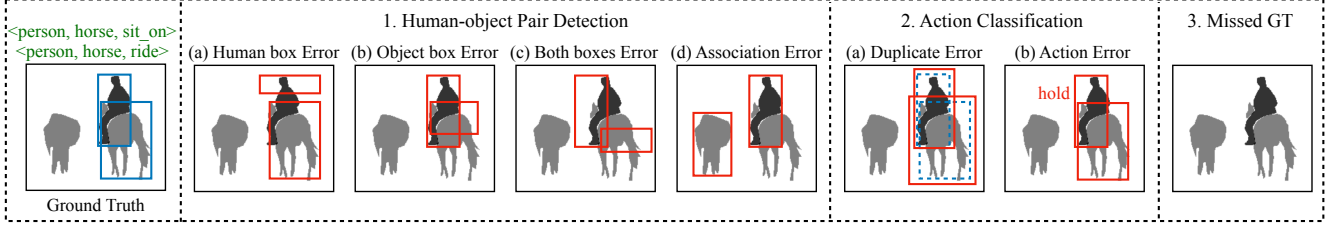


Figure 4: **Examples of different types of errors.** A human-object pair in the image has two occurring actions. We show seven sample HOI triplet predictions, corresponding to seven types of errors. For clearness, we only show one triplet prediction on each image (solid line). The dash line means there already exists a prediction with a higher confidence score.

Table 1: **Details of HOI detection models used in our analysis.**

Model	Venue	Architecture	Backbone	Object/Pair Detector	Action Classifier	$mAP$	
						HICO-DET	V-COCO
SCG [39]	ICCV 2021	two-stage	ResNet-50	FPN	GNN	33.3	49.4
UPT [40]	CVPR 2022		ResNet-50/101	DETR	Transformer	34.6 / 35.5	59.0 / 60.7
STIP [41]	CVPR 2022		ResNet-50	DETR	Transformer	31.6	67.2
CDN [38]	NeurIPS 2021	one-stage	ResNet-50/101	DETR	Transformer	34.4 / 35.1	61.7 / 63.9
GEN-VLKT [20]	CVPR 2022		ResNet-50/101	DETR	Transformer	35.8 / 36.5	62.4 / 63.6
QAHOI [9]	arXiv 2021		Swin-B/L	Deform.-DETR	Transformer	35.1 / 37.1	-

### 3.2. On the Human-object Pair Detection

For an HOI detector, whether one- or two-stage, it classifies the action label based on the human-object pair detection result. It is thus important to investigate whether the pair detection results are good enough so that the action classification module has the opportunity to recognize all possible action labels. To this end, we compute the recall value to evaluate a model’s ability to localize all ground-truth human-object pairs.

Specifically, we calculate the percentage of ground-truth human-object pairs that are contained in the detection results of human-object pairs, *without considering the action labels here*. Due to the multi-label nature, multiple ground-truth pairs can be matched to the same detected pair. In such a case, only one of them is considered as true positive and other duplicated detections will be considered as false positives. We finally report the average recall across the dataset.

As introduced in Section 2.3, for a two-stage HOI detector, the object detections (and thus the human-object pair detections) are filtered by the fixed threshold  $\tau_d$ . The number of detected pairs may vary from one detector to another. For a one-stage detector, it directly outputs a number of human-object pairs, *e.g.*, controlled by the number of queries in the DETR-like architectures [6, 38, 9].

Simply checking the recall value may not be sufficient since a detector can generate very noisy detections of human-object pairs. Although the recall value is high and the ground-truth annotations are all localized, they impose a significant burden on the action classification module to prune a lot of incorrect pairs. We therefore report the preci-

sion score as well on the dataset level.

### 3.3. On the Interaction Classification

Interaction classification is the second sub-task of HOI detection, which classifies actions based on detected human-object pairs. It needs to finish the following tasks.

#### Recognizing incorrect human-object pair detections.

For those incorrectly localized human-object pairs, they have no actual interactions and should be discarded in the final output, similar to the `background` category in the object detection task. Unlike the multi-label action classification, for this task, it is actually a *binary classification* problem. As we pointed out in Section 2.5, in V-COCO, if the classification scores for those actual interaction categories are very low, it indicates the human and object have no actual interactions. We therefore compute the classification score belonging to the negative class as  $1 - \max_i(p_i)$ , where  $p_i$  is the classification score of the  $i$ -th actual action class. We report the  $AP$  (average precision) score to avoid the selection of a threshold for the binary classification.

**Correct human-object pair detections.** For correctly localized pairs, there may be multiple action labels associated with them. We therefore compute the  $mAP$  score for the classification over all actual action categories, analyzing the performance for action classification. Note here we do not consider the detection scores for the correctly localized human-object pairs, disentangling the human-object pair detection and action classification tasks.

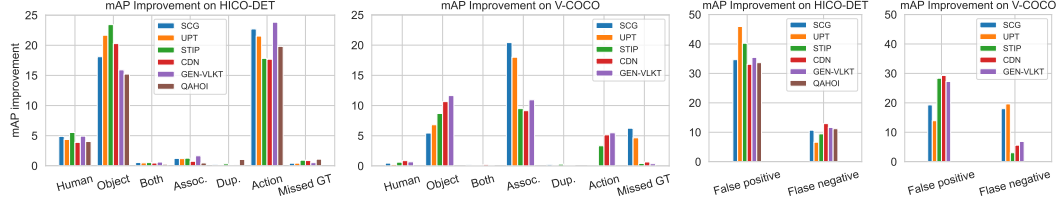


Figure 5:  $mAP$  improvement by fixing different types of errors on HICO-DET and VCOCO datasets.

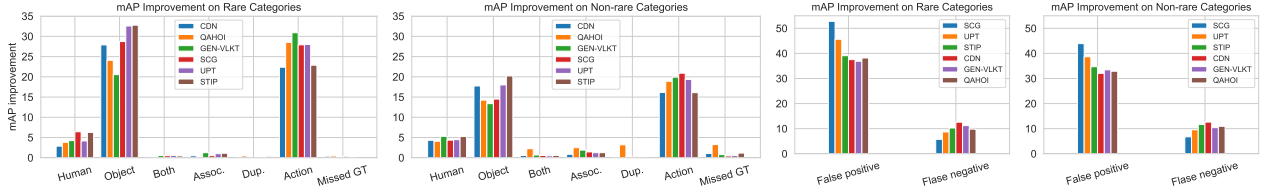


Figure 6:  $mAP$  improvement by fixing different types of errors for the rare and non-rare HOI categories on HICO-DET.

## 4. Diagnosis Results

### 4.1. Setup

In our analysis, we choose six popular HOI detection models, three two-stage and three one-stage, covering a wide range of design choices (e.g., backbone, object/pair detector, and action classifier). We use the code and model weights provided by the authors<sup>2</sup>. A summary of these models can be found in Table 1. QPIC [30], HOITR [44], and QAHOI [9] share similar model designs based on the DETR object detection model, we only investigate QAHOI here because it reports the highest  $mAP$ . We provide detailed introductions of these methods in the appendix.

### 4.2. $mAP$ Improvement

The  $mAP$  improvement for the seven types of errors and for the false positives and false negatives defined in Sec. 3.1 on both HICO-DET and V-COCO are shown in Fig. 5.

On HICO-DET, among all the seven errors across the human-object pair detection and action classification, we can find that all the HOI detectors benefit the most from fixing the object box errors and incorrect action classification errors. There is no significant difference between one-stage and two-stage HOI detectors. These can be attributed to two main factors. First, the HICO-DET dataset comprises a considerable number of actions, with a significant portion being multi-labeled, posing a challenge for the model to accurately distinguish between all actions. Secondly, as the detector is typically not pre-trained on the HICO-DET dataset, the model is susceptible to object box errors.

We also investigate the  $mAP$  improvement with respect to rare and non-rare HOI categories on HICO-DET dataset

in Fig. 6. An HOI category is considered as rare if it appears in the test set less than ten times. Otherwise, it is non-rare. We can observe that models tend to have more failures in rare HOI categories and fixing errors for rare HOI categories leads to larger  $mAP$  improvement. This is mainly due to the long-tail distribution of the HOI categories, making it hard for the model to perform well for the rare ones.

On the V-COCO dataset, errors are primarily concentrated on the object box errors and association errors of human and object bounding boxes. Particularly, two-stage HOI detectors exhibit a higher frequency of association errors compared to one-stage detectors, except for STIP. And the overall  $mAP$  improvement on V-COCO is not as notable as in the HICO-DET dataset. Part of the reason is that detectors are often pre-trained on the COCO dataset, which V-COCO is built upon. As a result, how to correctly associate the detections is more prominent than detecting them. Moreover, there are a relatively smaller and simpler set of actions in the V-COCO dataset compared with the more abstract actions present in HICO-DET (e.g., inspect, wield). It is worth noting that SCG [39] and UPT [40] do not exhibit action errors on the V-COCO dataset due to the pre-processing and suppression techniques.

From the last two figures of Fig. 5, we can see that for most HOI detectors on both HICO-DET and V-COCO, suppressing false positives brings significantly higher  $mAP$  improvement than false negatives, except for SCG [39] and UPT [40]. Note that the difference between “fixing false negatives” and “fixing missed GT” in Fig. 5 is due to different oracles used. We explain their differences in the supplementary material.

### 4.3. Human-object Pair Localization

We report the average recall and precision values for the human-object pair detection task on HICO-DET and V-

<sup>2</sup>Since the model on V-COCO is not available for QAHOI [9], we only report its diagnosis results on HICO-DET.

Table 2: Average recall and precision of one-stage and two-stage models on HICO-Det and V-COCO.

Arch.	Method	Backbone	HICO-Det				V-COCO			
			#Pairs	Recall	Precision	$mAP$	#Pairs	Recall	Precision	$mAP$
two-stage	SCG [39]	ResNet50	44	84.0	3.7	33.3	406	91.2	0.6	49.4
	UPT [40]	ResNet50	46	80.1	3.7	34.6	24	92.8	10.4	59.0
	UPT [40]	ResNet101	43	80.8	3.6	35.5	26	93.2	7.8	60.7
	STIP [41]	ResNet50	32	74.2	4.4	31.6	32	94	7.4	67.2
one-stage	CDN [38]	ResNet50	64	79.4	2.5	34.4	100	89.7	2.3	61.7
	GEN-VLKT [20]	ResNet50	64	81.1	2.6	35.8	64	88.5	3.5	62.4
	GEN-VLKT [20]	ResNet101	64	81.8	2.6	36.5	64	89.5	3.4	63.6
	QAHOI [9]	SwinB	64	81.6	1.6	35.1	-	-	-	-

Table 3:  $AP$  score of binary classification and action  $mAP$  on HICO-DET and V-COCO. The neg.  $AP$  captures the performance of classifying the negative human-object pairs (without actual interactions). The act.  $mAP$  is for the correctly localized pairs.

Method	Backbone	HICO-DET		VCOCO	
		neg. $AP$	Act. $mAP$	neg. $AP$	Act. $mAP$
SCG [39]	ResNet50	91.8	46.5	99.0	63.48
UPT [40]	ResNet50	91.9	32.5	99.2	64.46
UPT [40]	ResNet101	91.8	32.4	99.4	64.72
STIP [41]	ResNet50	91.7	51.1	97.8	82.1
CDN [38]	ResNet50	67.8	54.3	96.8	76.64
GEN-VLKT [20]	ResNet50	67.3	49.6	79.2	75.7
GEN-VLKT [20]	ResNet101	70.0	52.5	86.7	77.2
QAHOI [9]	SwinB	84.1	53.1	-	-

COCO datasets in Tab. 2.

Perhaps a little surprisingly, although two-stage detectors exhaustively pair detected human and object bounding boxes, the number of detected pairs is lower than the one-stage counterparts. Moreover, both the two-stage models’ recall and precision are slightly higher than the one-stage ones (except for STIP and GEN-VLKT). At the same time, the recall values for both one-stage and two-stage methods are notably lower than 100. As a result, the missed detection of the ground-truth pairs has no opportunity to be fed into the action classification module, leading to low  $mAP$ .

Besides, the recall of the HOI detectors on V-COCO is significantly higher than on HICO-DET (around 90), which leads to higher HOI detection  $mAP$  scores. For HICO-DET, we compare recall and precision for rare and non-rare categories in Table 4. We can see that both recall and precision scores of rare categories are lower than the non-rare ones for both one-stage and two-stage methods.

As introduced in Sec. 2.3, the NMS is applied over the final HOI detections, which explains why the number of detected pairs is higher than the two-stage counterparts. To make the number of pairs comparable, we apply NMS to

remove the duplicate human-object pair detections for one-stage models. We also lower the detection threshold  $\tau_d$  of two-stage models so that more pairs can be generated. Due to limited space, the results are put in the appendix.

#### 4.4. Interaction Classification

We first report  $AP$  of classifying negative human-object pairs to see if the model is able to give low confidence scores to incorrect localized human-object pairs. From results of “neg.  $AP$ ” in Tab. 3, one-stage methods perform well in this task. From the results of action  $mAP$  in Tab. 3, we can see that although two-stage models have relatively higher pair recall, their interaction classification heads are hard to correctly classify all the actions. One-stage models have more confident scores towards correct interaction predictions, leading to higher action  $mAP$ . The performance of human-object pair detection and interaction classification get canceled. As a result, the  $mAP$  HOI detection for both two-stage and one-stage models are roughly the same.

In Table 4, we can see that one-stage methods tend to work better than two-stage methods. Particularly, GEN-VLKT [20] has notably better action classification ability over rare categories, which is mainly due to its usage of pre-trained visual-language model CLIP [28]. At the same time, the action  $mAP$  scores of rare HOI categories are significantly lower than non-rare ones for both one-stage and two-stage ones. It suggests that the bottleneck of HOI detection for rare HOI categories lies in both the human-object pair localization and interaction classification.

## 5. Discussions

**Two-stage vs. one-stage HOI detection models.** Although in terms of  $mAP$ , there is no clear advantage of one paradigm over the other, our diagnosis method allows us to derive more insights about such two types of HOI detectors. The results of  $mAP$  improvement in Fig. 5 show that both two-stage and one-stage detectors do not have a significant difference. Both of them struggle with the object error and action error on the HICO-DET dataset and most of the er-

Table 4: **Pair localization results and action  $mAP$  for Rare and Non-rare HOI categories on HICO-DET.**

Arch.	Method	Backbone	Non-rare Categories			Rare Categories		
			Pair Rec.	Pair Prec.	action $mAP$	Pair Rec.	Pair Prec.	action $mAP$
two-stage	SCG [39]	ResNet50	84.3	3.60	41.4	72.9	0.16	13.0
	UPT [40]	ResNet50	78.6	1.12	26.3	70.6	0.06	7.5
	UPT [40]	ResNet101	80.0	1.21	26.7	72.3	0.07	7.5
	STIP [41]	ResNet50	73.7	1.50	40.1	66.8	0.08	12.6
one-stage	CDN [38]	ResNet50	77.4	0.79	44.5	72.3	0.04	12.8
	GEN-VLKT [20]	ResNet50	79.5	0.81	43.1	71.7	0.04	19.5
	GEN-VLKT [20]	ResNet101	80.5	0.83	45.6	74.2	0.05	22.4
	QAHOI [9]	Swin-B	81.0	0.53	45.0	70.4	0.03	10.5

rors are about false positives.

But interestingly, Table 2 reveals that two-stage models generally produce human-object pairs with similar recall but higher precision values, indicating the detections are less noisy. At the same time, according to Table 3, while two-stage models are better at recognizing negative human-object pairs without actual interactions, they struggle to correctly recognize the actual interactions for those correctly localized human-object pairs.

**Different backbones.** A stronger backbone can help improve the  $mAP$  score of HOI detection. But where is the improvement from? The answers seem to vary for different models according to Fig. 7. For instance, ResNet101 can help reduce object error and action error, which are the two most significant errors, for UPT on HICO-DET, it is the opposite for the GEN\_VLKT model. Even for UPT itself, the trend is different on HICO-DET and V-COCO. In terms of human-object pair detection, ResNet101 improves the recall while keeping the precision unchanged for both UPT and GEN\_VLKT, meaning more ground-truth pairs can be detected. For action classification, the ResNet101 is not helpful for UPT, whereas it significantly improves GEN\_VLKT, enhancing both the negative pair classification and actual interaction recognition.

**Performance over HICO-DET and V-COCO.** The  $mAP$  on V-COCO is higher than HICO-DET. According to our diagnosis, the major errors on two datasets are consistent, where they are mostly from object error and action error. False positives are more significant than false negatives. For the human-object pair detection, the recall on the V-COCO is significantly higher (please refer to our supplementary material for more details) while the precision score is still low. At the same time, HOI detectors generally perform significantly better on V-COCO than HICO-DET in terms of classifying the negative human-object pairs and recognizing the actual interactions between humans and objects.

**Human-object pair detection vs. action classification.** The  $mAP$  improvement diagnosis suggests that improving one of them can reduce the errors and improve the final accuracy. Similarly, in Table 2, we can see that the recall on

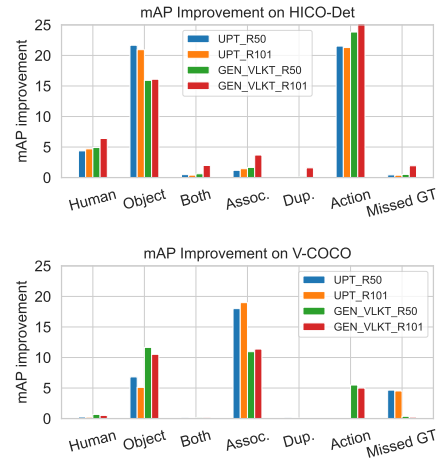


Figure 7:  **$mAP$  improvement** of different backbones on HICO-DET and VCOCO.

both datasets is still much lower than 100, implying a lot of ground-truth pairs can not be detected. At the same time, the results in Table 3 show that correctly recognizing the actual interactions is still a challenging problem.

Practically, human-object pair largely depends on the progress of generic single-object detection, which is a long-standing problem in computer vision and has attracted a significant amount of research attention. The performance on standard benchmarks is saturated. In contrast, interaction recognition in HOI detection is a multi-label classification problem, which has not yet been extensively studied.

## 6. Conclusion

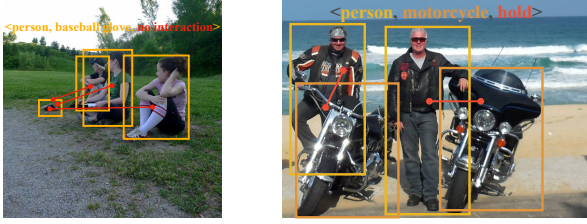
In this paper, we introduced the first diagnosis toolbox for HOI detectors. We first defined a set of errors across the pipeline of HOI detection and report the  $mAP$  improvement by fixing each of them using an oracle. In addition to this holistic study, we also delve into the human-object pair detection and interaction classification tasks separately. Detailed analyses are reported on both HICO-DET and V-COCO over six state-of-the-art HOI detectors. We believe our diagnosis toolbox and analysis results will be helpful for fostering future research in this direction.



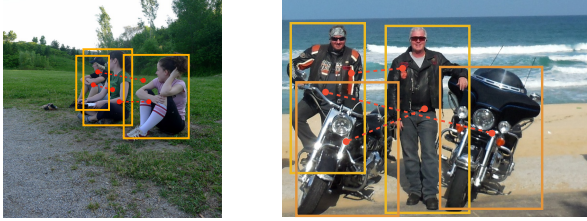
## References

- [1] Peter Anderson, Xiaodong He, Chris Buehler, Damien Teney, Mark Johnson, Stephen Gould, and Lei Zhang. Bottom-up and top-down attention for image captioning and visual question answering. In *CVPR*, 2018. 1
- [2] Jyoti Aneja, Aditya Deshpande, and Alexander G Schwing. Convolutional image captioning. In *CVPR*, 2018. 1
- [3] Stanislaw Antol, Aishwarya Agrawal, Jiasen Lu, Margaret Mitchell, Dhruv Batra, C Lawrence Zitnick, and Devi Parikh. Vqa: Visual question answering. In *ICCV*, 2015. 1
- [4] Daniel Bolya, Sean Foley, James Hays, and Judy Hoffman. TIDE: A general toolbox for identifying object detection errors. In *ECCV*, 2020. 1, 2, 4, 11
- [5] Andrew Brown, Weidi Xie, Vicky Kalogeiton, and Andrew Zisserman. Smooth-ap: Smoothing the path towards large-scale image retrieval. In *Computer Vision—ECCV 2020: 16th European Conference, Glasgow, UK, August 23–28, 2020, Proceedings, Part IX 16*, 2020. 1
- [6] Nicolas Carion, Francisco Massa, Gabriel Synnaeve, Nicolas Usunier, Alexander Kirillov, and Sergey Zagoruyko. End-to-end object detection with transformers. In *ECCV*, 2020. 5
- [7] Yu-Wei Chao, Yunfan Liu, Xieyang Liu, Huayi Zeng, and Jia Deng. Learning to detect human-object interactions. 2018. 1, 3, 4
- [8] Yu-Wei Chao, Zhan Wang, Yugeng He, Jiaxuan Wang, and Jia Deng. HICO: A benchmark for recognizing human-object interactions in images. In *ICCV*, 2015. 1, 3, 4
- [9] Junwen Chen and Keiji Yanai. QAHOI: Query-based anchors for human-object interaction detection. *arXiv preprint arXiv:2112.08647*, 2021. 5, 6, 7, 8, 12, 13
- [10] Shuo Chen, Pascal Mettes, and Cees GM Snoek. Diagnosing errors in video relation detectors. In *BMVC*, 2021. 2
- [11] Yang Feng, Lin Ma, Wei Liu, and Jiebo Luo. Unsupervised image captioning. In *CVPR*, 2019. 1
- [12] Chen Gao, Jiarui Xu, Yuliang Zou, and Jia-Bin Huang. DRG: Dual relation graph for human-object interaction detection. In *ECCV*, 2020. 1
- [13] Saurabh Gupta and Jitendra Malik. Visual semantic role labeling. *arXiv preprint arXiv:1505.04474*, 2015. 1, 2, 3, 4
- [14] Tanmay Gupta, Alexander Schwing, and Derek Hoiem. No-frills human-object interaction detection: Factorization, layout encodings, and training techniques. In *ICCV*, 2019. 1
- [15] Derek Hoiem, Yodsawalai Chodpathumwan, and Qieyun Dai. Diagnosing error in object detectors. In *ECCV*, 2012. 2
- [16] Huaizu Jiang, Xiaojian Ma, Weili Nie, Zhiding Yu, Yuke Zhu, and Anima Anandkumar. Bongard-hoi: Benchmarking few-shot visual reasoning for human-object interactions. In *cvpr*, 2022. 1
- [17] Mert Kilickaya and Arnold Smeulders. Diagnosing rarity in human-object interaction detection. In *CVPR*, 2020. 2
- [18] Guang Li, Linchao Zhu, Ping Liu, and Yi Yang. Entangled transformer for image captioning. In *ICCV*, 2019. 1
- [19] Yong-Lu Li, Hongwei Fan, Zuoyu Qiu, Yiming Dou, Liang Xu, Hao-Shu Fang, Peiyang Guo, Haisheng Su, Dongliang Wang, Wei Wu, et al. Discovering a variety of objects in spatio-temporal human-object interactions. *arXiv preprint arXiv:2211.07501*, 2022. 1
- [20] Yue Liao, Aixi Zhang, Miao Lu, Yongliang Wang, Xiaobo Li, and Si Liu. Gen-vlkt: Simplify association and enhance interaction understanding for hoi detection. In *CVPR*, 2022. 1, 5, 7, 8, 12, 13
- [21] Tsung-Yi Lin, Michael Maire, Serge Belongie, James Hays, Pietro Perona, Deva Ramanan, Piotr Dollár, and C Lawrence Zitnick. Microsoft coco: Common objects in context. In *ECCV*, 2014. 2, 3
- [22] Xinpeng Liu, Yong-Lu Li, and Cewu Lu. Highlighting object category immunity for the generalization of human-object interaction detection. In *AAAI*, 2022. 2
- [23] Xinpeng Liu, Yong-Lu Li, Xiaoqian Wu, Yu-Wing Tai, Cewu Lu, and Chi-Keung Tang. Interactiveness field in human-object interactions. In *cvpr*, 2022. 1
- [24] Jiasen Lu, Jianwei Yang, Dhruv Batra, and Devi Parikh. Hierarchical question-image co-attention for visual question answering. *Advances in neural information processing systems*, 2016. 1
- [25] Shuailei Ma, Yuefeng Wang, Shanze Wang, and Ying Wei. Fgahoi: Fine-grained anchors for human-object interaction detection. *arXiv preprint arXiv:2301.04019*, 2023. 1
- [26] Tony Ng, Vassileios Balntas, Yurun Tian, and Krystian Mikolajczyk. Solar: second-order loss and attention for image retrieval. In *Computer Vision—ECCV 2020: 16th European Conference, Glasgow, UK, August 23–28, 2020, Proceedings, Part XXV 16*, 2020. 1
- [27] Filip Radenović, Giorgos Tolias, and Ondřej Chum. Fine-tuning cnn image retrieval with no human annotation. *IEEE TPAMI*, 2018. 1
- [28] Alec Radford, Jong Wook Kim, Chris Hallacy, Aditya Ramesh, Gabriel Goh, Sandhini Agarwal, Girish Sastry, Amanda Askell, Pamela Mishkin, Jack Clark, et al. Learning transferable visual models from natural language supervision. In *International Conference on Machine Learning*, pages 8748–8763. PMLR, 2021. 7, 14
- [29] Kevin J Shih, Saurabh Singh, and Derek Hoiem. Where to look: Focus regions for visual question answering. In *CVPR*, pages 4613–4621, 2016. 1
- [30] Masato Tamura, Hiroki Ohashi, and Tomoaki Yoshinaga. Qpic: Query-based pairwise human-object interaction detection with image-wide contextual information. In *CVPR*, 2021. 6
- [31] Marvin Teichmann, Andre Araujo, Menglong Zhu, and Jack Sim. Detect-to-retrieve: Efficient regional aggregation for image search. In *Proceedings of the IEEE/CVF Conference on Computer Vision and Pattern Recognition*, 2019. 1
- [32] Oytun Ulutan, ASM Iftekhar, and Bangalore S Manjunath. VSGNet: Spatial attention network for detecting human object interactions using graph convolutions. In *CVPR*, 2020. 1
- [33] Oriol Vinyals, Alexander Toshev, Samy Bengio, and Dumitru Erhan. Show and tell: Lessons learned from the 2015 mscoco image captioning challenge. *IEEE TPAMI*, 2016. 1
- [34] Peng Wang, Qi Wu, Chunhua Shen, Anthony Dick, and Anton Van Den Hengel. Fvqa: Fact-based visual question answering. *IEEE TPAMI*, 2017. 1

- [35] Xiaoqian Wu, Yong-Lu Li, Xinpeng Liu, Junyi Zhang, Yuzhe Wu, and Cewu Lu. Mining cross-person cues for body-part interactiveness learning in hoi detection. In *Computer Vision–ECCV 2022: 17th European Conference, Tel Aviv, Israel, October 23–27, 2022, Proceedings, Part IV*, 2022. 1
- [36] Zecheng Yu, Yifei Huang, Ryosuke Furuta, Takuma Yagi, Yusuke Goutsu, and Yoichi Sato. Fine-grained affordance annotation for egocentric hand-object interaction videos. In *WACV*, 2023. 1
- [37] Hangjie Yuan, Jianwen Jiang, Samuel Albanie, Tao Feng, Ziyuan Huang, Dong Ni, and Mingqian Tang. Rlip: Relational language-image pre-training for human-object interaction detection. In *Advances in Neural Information Processing Systems*. 1
- [38] Aixi Zhang, Yue Liao, Si Liu, Miao Lu, Yongliang Wang, Chen Gao, and Xiaobo Li. Mining the benefits of two-stage and one-stage hoi detection. In *NeurIPS*, 2021. 1, 5, 7, 8, 11, 12, 13
- [39] Frederic Z Zhang, Dylan Campbell, and Stephen Gould. Spatially conditioned graphs for detecting human-object interactions. In *ICCV*, 2021. 1, 5, 6, 7, 8, 12, 13, 14
- [40] Frederic Z Zhang, Dylan Campbell, and Stephen Gould. Efficient two-stage detection of human-object interactions with a novel unary-pairwise transformer. In *CVPR*, 2022. 5, 6, 7, 8, 12, 13, 14
- [41] Yong Zhang, Yingwei Pan, Ting Yao, Rui Huang, Tao Mei, and Chang-Wen Chen. Exploring structure-aware transformer over interaction proposals for human-object interaction detection. In *CVPR*, 2022. 1, 5, 7, 8, 12, 13
- [42] Xubin Zhong, Changxing Ding, Zijian Li, and Shaoli Huang. Towards hard-positive query mining for detr-based human-object interaction detection. In *ECCV*, 2022. 1
- [43] Penghao Zhou and Mingmin Chi. Relation parsing neural network for human-object interaction detection. In *ICCV*, 2019. 1
- [44] Cheng Zou, Bohan Wang, Yue Hu, Junqi Liu, Qian Wu, Yu Zhao, Boxun Li, Chenguang Zhang, Chi Zhang, Yichen Wei, et al. End-to-end human object interaction detection with hoi transformer. In *CVPR*, 2021. 6



(a) current annotations



(b) missing annotations (the dashed lines and bounding box)

Figure 8: **An additional example of the missing annotations of the `no_interaction` HOI class.** On the right, we show missing `no_interaction` labels and missing bounding box using dashed lines and bounding boxes, respectively.

## A. Elaboration on `no_interaction` Class in HICO-DET

We would like to emphasize that not computing the  $mAP$  for the `no_interaction` HOI category does not change an HOI detector’s output to ignore the human-object pairs that have no interactions nor do we underestimate the detector’s accuracy in our diagnosis. First, we do not remove the `no_interaction` label in the model’s output so there is no need to re-train the model. An HOI model is still able to tell that a human-object pair has no interactions, which we will discuss in detail in Section 3.3. Second, if the model incorrectly classifies a human-object pair that has no interaction as having an actual interaction (e.g., `ride bicycle`), such an incorrect output will be considered as a false positive. Similarly, incorrectly classifying the pair of `ride bicycle` as `no_interaction` will reduce the number of true positives. Both of such errors will lead to a lower  $mAP$  that correctly measures the model’s accuracy.

## B. Details of fixing errors using oracles

In this section, we provide details of how we fix errors according to different oracles. We show visualization examples of how we fix different types of errors in Fig. 9.

**Fixing the human-object pair detection errors.** It involves four oracles.

- **Human box oracle:** Fix the human box detection and action label, making it a true positive. If duplicates are made, suppress the lower-scoring prediction.

- **Object box oracle:** Fix such false positives in a similar way as introduced in the previous step.
- **Human-object boxes oracle:** Since both boxes are incorrect, we cannot decide which ground truth triplet the detection is attempting to match. We just remove this kind of false positive prediction.
- **Association oracle:** Correct the pair association and action label, making it a true positive. If duplicates are made in this way, suppress the lower-scoring prediction.

**Fixing action classification errors.** In this case, we fix false positives caused by action error or duplicate error.

- **Action classification oracle:** Fix the action label to make it a true positive. If duplicates are made in this way, suppress the lower-scoring prediction.
- **Duplicate oracle:** We directly remove all duplicate predictions.
- **Missing oracle:** Note that, after fixing all the above errors, there are still ground truth triplets that are not matched with any predictions, the number of which is the number of missed ground truth triplets. We reduce the number of ground-truth HOI triplets in the  $mAP$  calculation by the number of missed ground-truth triplets.

**Fixing other Error types.**

- **False positive oracle:** Remove all false positive predictions.
- **False negative oracle:** Set the number of ground truth triplets to the number of true positive predictions.

**Oddities of  $mAP$  improvement.** Similar to [4], the  $mAP$  improvement in our case has the same issue that the summation of  $\Delta mAP$  of different error types does not lead to  $100 - mAP$ . For example, in Fig. 5 of the main paper, adding  $mAP$  of CDN [38] with  $\Delta mAP_{FP}$  and  $\Delta mAP_{FN}$  ( $34.4+33.1+12.94$ ) yields 80.44, not 100. As pointed out in [4], the reason is that fixing different errors at once gives a larger  $mAP$  improvement than fixing each error on its own.

## C. Pair localization results

Pair localization results on the HICO-DET and V-COCO datasets are shown in Tab. 5 and 6. We can see that recall values for all methods on the two datasets are lower than 100. The pair detection task of V-COCO dataset is easier than that of HICO-DET dataset, resulting in higher recall values. And we can draw the conclusion that neither increasing nor decreasing the number of pairs leads to a significant enhancement of the final  $mAP$ , indicating that correct pair detection is still challenging.

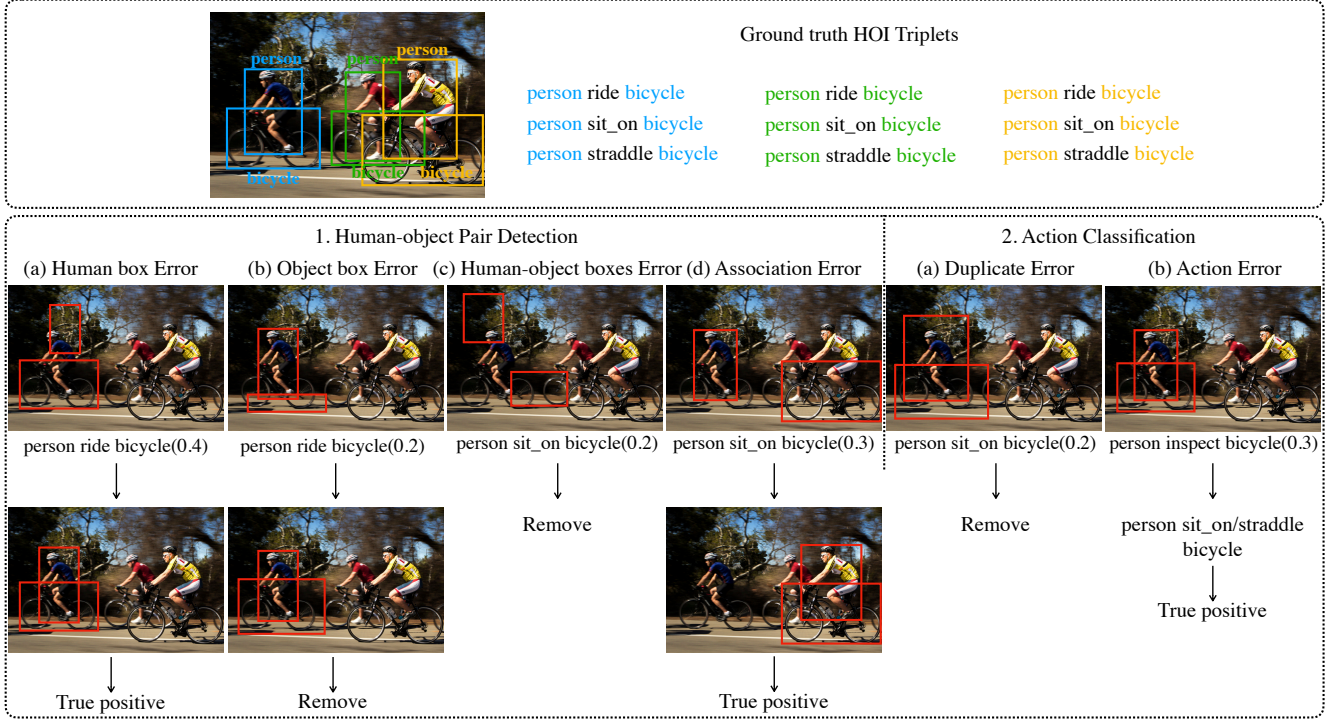


Figure 9: Examples of different error types in real images and how we fix them using oracles. There are three human-object pairs in the ground truth with three interactions between each pair. There are six predicted triplets in the second row, corresponding to six different error types. We fix each of them into true positives and remove duplicates afterward.

Table 5: Average recall and precision of one-stage and two-stage models on HICO-DET dataset.

Arch.	Method	Backbone	Original Models				w/ NMS or lower detection threshold $\tau_d$			
			#Pairs	Recall	Precision	$mAP$	#Pairs	Recall	Precision	$mAP$
two-stage	SCG [39]	ResNet50	44	84.0	3.7	33.3	78 (34)	86.9 (2.9)	2.2 (-1.5)	33.3 (0.0)
	UPT [40]	ResNet50	46	80.1	3.7	34.6	62 (16)	81.7 (1.6)	2.5 (-1.2)	34.8 (0.2)
	UPT [40]	ResNet101	43	80.8	3.6	35.5	57 (14)	82.3 (1.5)	2.8 (-0.8)	35.6 (0.1)
	STIP [41]	ResNet50	32	74.2	4.4	31.6	64 (32)	75.6 (1.4)	2.3 (-1.9)	31.1 (-0.5)
one-stage	CDN [38]	ResNet50	64	79.4	2.5	34.4	26 (-38)	72.0 (-7.4)	5.5 (3.0)	34.4 (0.0)
	GEN-VLKT [20]	ResNet50	64	81.1	2.6	35.8	27 (-37)	78.7 (-2.4)	5.5 (1.9)	36.0 (0.2)
	GEN-VLKT [20]	ResNet101	64	81.8	2.6	36.5	28 (-36)	79.5 (-2.3)	5.4 (1.8)	36.5 (0.0)
	QAHOI [9]	SwinB	64	81.6	1.6	35.1	45 (-19)	79.7 (-1.4)	3.0 (0.7)	35.2 (0.1)

As introduced in Sec. 2.3, the NMS is applied over the final HOI detections, which explains why the number of detected pairs is higher than the two-stage counterparts.

To make the number of pairs comparable, we apply NMS to remove the duplicate human-object pair detections for one-stage models. We also lower the detection threshold  $\tau_d$  of two-stage models so that more pairs can be generated.

The right parts of Tab. 5 and 6 show that as the number of pairs increases, recall improves while precision declines. However, neither increasing nor decreasing the number of pairs leads to a significant enhancement of the final  $mAP$ . Thus, we can conclude that accurate pair detection is still a challenge for both one-stage and two-stage HOI detectors.

## D. Models Used in Our Diagnosis

We choose six popular HOI detection models including three one-stage and three two-stage detectors for our diagnosis. We give a brief summary for each model we used.

**SCG [39]** solves the HOI detection problem by graphical neural networks with a two-stage design. It designs condition messages between pairs of nodes on their spatial relationships.

**UPT [40]** proposes an Unary-Pairwise Transformer architecture, but makes it a two-stage model that exploits unary and pairwise representations for HOIs.

**STIP [41]** is a two-stage method that uses a Transformer-



Table 6: Average recall and precision of one-stage and two-stage models on V-COCO dataset.

Arch.	Method	Backbone	Original Models				w/ NMS or lower detection threshold $\tau_d$			
			#Pairs	Recall	Precision	$mAP$	#Pairs	Recall	Precision	$mAP$
two-stage	SCG [39]	ResNet50	406	91.2	0.6	49.4	98 (-308)	90.6 (-0.6)	2.5 (1.9)	49.5 (0.1)
	UPT [40]	ResNet50	24	92.8	10.4	59.0	50 (26)	94.8 (2)	5.2 (-5.2)	59.2 (0.2)
	UPT [40]	ResNet101	26	93.2	7.8	60.7	55 (29)	94.1 (0.9)	6.1 (-1.7)	60.9 (0.2)
	STIP [41]	ResNet50	32	94	7.4	67.2	23 (-9)	92.9 (1.4)	10.4 (3)	67.1 (-0.1)
one-stage	CDN [38]	ResNet50	100	89.7	2.3	61.7	40 (-60)	88.8 (-0.9)	5.5 (3.2)	61.6 (-0.1)
	GEN-VLKT [20]	ResNet50	64	88.5	3.5	62.4	39 (-25)	87.3 (-1.2)	5.6 (2.1)	62.4 (0.0)
	GEN-VLKT [20]	ResNet101	64	89.5	3.4	63.6	37 (-27)	88.1 (-1.4)	5.5 (2.1)	63.6 (0.0)

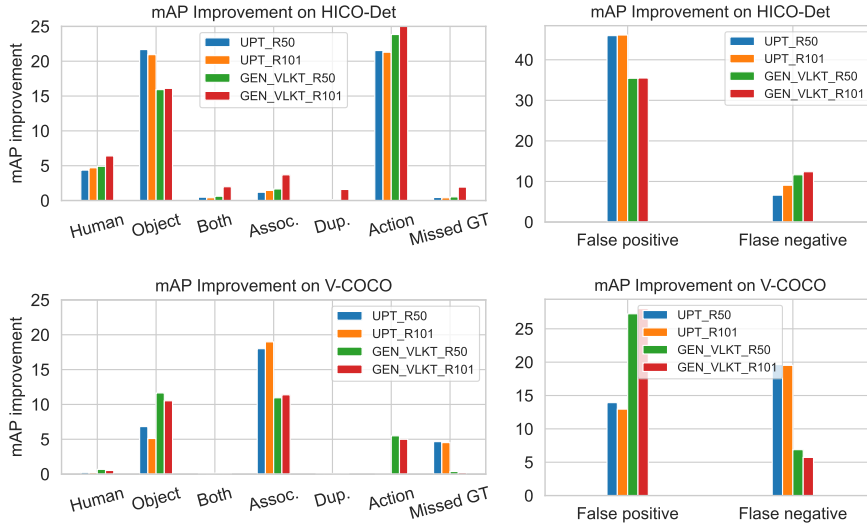


Figure 10:  $mAP$  improvement of UPT [40] and GEN-VLKT [20] with different backbones.



Figure 11: Visualization of errors of SCG [39] and UPT [40] on the V-COCO dataset. We show the ground truth triplet (in cyan color) and the error type of the prediction (red characters) for each image. The red boxes represent predictions.

based detector to generate interaction proposals first, and then transforms the nonparametric interaction proposals into HOI predictions via a structure-aware Transformer.

CDN [38] proposes a one-stage method with disentangling human-object detection and interaction classification in a cascade manner. It first uses a human-object pair generator and then designs an isolated interaction classifier to classify each human-object pair.

QAHOI [9] proposes a transformer-based one-stage method, which leverages a multi-scale architecture to extract features from different scales and uses query-based anchors to predict human-object pairs and their interactions as triplets.

GEN-VLKT [20] follows the one-stage cascaded manner of CDN, and designs guided embeddings and instance guided embeddings to generate HOI instances. Besides, it

proposes a Visual-Linguistic Knowledge Transfer training strategy for better interaction understanding by transferring knowledge from a pre-trained model CLIP [28].

## E. Visualization of errors on V-COCO

We randomly choose test images from the V-COCO dataset to see the predictions of SCG [39] and UPT [40], as shown in Fig 11. Since these two methods use the postprocessing method, there are no action errors in the predictions.

## F. $mAP$ improvement for different backbones

We show full results of  $mAP$  improvement on HICO-DET and V-COCO datasets regarding different backbone choices in Fig. 10. From the results, we can find that although a stronger backbone leads to better performance, the detailed  $mAP$  improvement does not show a significant difference regarding different backbones.

## G. Human Detection

Previous analysis of  $mAP$  improvement shows that the human error is not as significant as the generic objects. Here, we examine the recall of human detection. On the HICO-DET dataset, the average recall of human detection is 91.5, while the average recall of all object categories is 88.0<sup>3</sup>. We can see that human detection is easier but the performance is still far from satisfactory.

---

<sup>3</sup>Since the annotations of objects are not complete as we pointed out in Section 3.1 in the main paper, the precision is not reliable.